Biorheology 43 (2006) 45–55
IOS Press

Micropatterned polymer surfaces improve retention of endothelial cells exposed to flow-induced shear stress

Sachin C. Daxini [a,*], Jason W. Nichol [b,c,*], Alisha L. Sieminski [b,c], Geoffrey Smith [d], Keith J. Gooch [b,e] and V. Prasad Shastri [c,d,f,g,**]

[a] *Masters in Biotechnology Program, School of Engineering and Applied Science, University of Pennsylvania, Philadelphia, PA, USA*
[b] *Department of Bioengineering, University of Pennsylvania, Philadelphia, PA, USA*
[c] *Institute for Medicine and Engineering, University of Pennsylvania, Philadelphia, PA, USA*
[d] *Department of Materials Science and Engineering, University of Pennsylvania, Philadelphia, PA, USA*
[e] *Department of Biomedical Engineering, Ohio State University, Columbus, OH, USA*
[f] *Joseph Stokes Jr. Research Center, Children's Hospital of Philadelphia, USA*
[g] *Department of Biomedical Engineering, Vanderbild University, Nashville, TN, USA*

Received 24 May 2005
Accepted in revised form 8 December 2005

Abstract. The use of synthetic polymeric vascular grafts is limited by the thrombogenecity of most biomaterials. Efforts to reduce thrombogenicity by seeding grafts with endothelial cells, the natural non-thrombogenic lining of blood vessels, have been thwarted by flow-induced cell detachment. We hypothesized that by creating well-defined micro-textured patterns on a surface, fluid flow at the surface can be altered to create discrete regions of low shear stress. We further hypothesized that, due to reduced shear stress, these regions will serve as sanctuaries for endothelial cells and promote their retention. To test these hypotheses, well-defined micro-textured polyurethane (PU) surfaces consisting of arrays of parallel 95-micron wide and 32-micron deep channels were created using an etched silicon template and solvent casting techniques. Based on computational fluid dynamics, under identical bulk flow conditions, the average local shear stress in the channels (46 dyn/cm^2) was 28% lower than unpatterned surfaces (60 dyn/cm^2). When PU surfaces pre-seeded with endothelial cells (EC) were exposed to the same bulk flow rate, EC retention was significantly improved on the micropatterned surfaces relative to un-patterned surfaces (92% vs. 58% retention).

Keywords: Endothelial cells, microfabrication, retention, computational fluid dynamics, vascular grafts, tissue engineering

[*] Equally contributing authors.
[**] Address for correspondence: Dr. V. Prasad Shastri, 5824 Stevenson Center, Department of Biomedical Engineering, Vanderbilt University, Nashville, TN 37232, USA. Tel.: + 615 322 8005; Fax: +1 615 343 7919; E-mail: Prasad.Shastri@vanderbilt.edu.

1. Introduction

Occlusion of arteries due to plaque deposition and thrombosis results in reduced blood flow. Depending on the arteries affected, occlusion may lead to peripheral vascular disease, stroke or angina pectoris/myocardial infarct, making it the single largest cause of death in the United States. Treatment options for restoring flow through occluded arteries include thrombolytic agents, mechanical means of opening lumens such as balloon angioplasty and stenting, as well as bypassing the blocked segment, which is frequently the preferred option [3]. Typically, autografts are used to bypass the occluded artery although their harvest is associated with donor site morbidity and, in some cases, is precluded by lack of appropriate available donor vessels. Synthetic polymeric grafts are therefore, attractive options, as polymer supply and fabrication are not limiting factors. Expanded polytetrafluoroethylene (ePTFE) and Dacron are used clinically as grafts for large-diameter vessels (>6 mm) but when used for small-diameter grafts (<6 mm), intimal hyperplasia at the anastomoses, attributed to compliance mismatch between the graft and native vessel, and thrombus formation, attributed to the thrombogenecity of the synthetic polymers used, result in an unacceptable patency (reviewed in [18]). Use of polyurethanes (PU), which have compliance values closer to native tissue [10], may eliminate compliance mismatch associated with relatively rigid materials like PTFE and Dacron, but thrombus formation is still a concern.

Endothelial cells (EC) constitute the natural non-thrombogenic surface of blood vessels. Since the 1970s, a number of investigators have explored seeding EC on the luminal surface of synthetic grafts to reduce the thrombogenicity of synthetic grafts (reviewed in [18]). Though an attractive idea, loss of endothelial cells from the grafts upon exposure to flow-induced shear stress remains a barrier. Numerous methods to increase adhesion and retention of EC to a polymeric surface have been explored, including covalent modification [12,13,15,16], adsorption of native [4,16] or engineered [11] proteins, prior seeding with smooth muscle cells [17], use of pressure [5] or electrostatic forces [2] to facilitate endothelial seeding, modification of endothelial cells [5], and mechanical preconditioning of seeded cells [1,6].

To address the problem of endothelial cell loss from pre-seeded synthetic vascular grafts, we have explored non-chemical modification of the graft surface. Specially, we hypothesized that by creating well-defined micro-patterns on a surface, fluid flow at the surface can be altered to create discrete regions of lowered shear stress. We further hypothesized that, due to reduced shear stress, these regions will serve as sanctuaries for EC and promote their retention. Here we demonstrate that by creating a simple surface micro-architecture composed of an array of channels, local regions of lowered shear stress are produced, leading to improved EC retention. We believe that this non-chemical micro-patterning approach may present a novel way to engineer and improve the patency of vascular grafts derived from a wide range of synthetic polymers and can be used independently or in conjunction with chemical modification of the surface.

2. Materials and methods

2.1. Preparation of patterned template

A negative impression of the desired pattern of parallel channels was created on a $3''$ silicon wafer using standard lithography techniques. The desired pattern was generated using AutoCAD-2000 and then transferred to a Ferrox mask. The wafer was then coated with AZ 5200-E positive photoresist (AZ Electronic Materials, Somerville, NJ) and the desired pattern was then transferred to the resist surface by exposing the resist layer to UV radiation via a Ferrox mask bearing the desired pattern to depolymerize

the resist in the exposed regions. The depolymerized resist was then removed by solubilization in a AZ 917 MIF developer (AZ Electronic Materials) and the exposed regions of the wafer were coated with a nitride layer by vacuum deposition. The unexposed resist was then removed using an AZ Kwik Strip stripper solution (AZ Electronic Materials) and exposed silicon surface was subjected to anisotropic etching using potassium hydroxide.

2.2. Preparation of micro-patterned polyurethane (PU) films

The silicon wafer template was used to pattern medical grade PU films by a solvent casting technique. In brief, a warm (45°C) solution of segmented polyether urethane (75 mg/ml ST1882, Stevens Urethane, Easthampton, MA) in tetrahydrofuran (Aldrich, St. Louis, MO) was deposited on silicon wafer templates in a drop-wise manner until complete surface coverage was achieved. The film was air-dried for 12 hours and released from the silicon substrate by soaking in isopropanol, which also served to remove residual tetrahydrofuran. Non-patterned PU films were made by a similar casting procedure on un-patterned 3″-silicon wafer substrates. PU films were sterilized by immersion in 70% ethanol for 30 minutes and then dried overnight under the UV light of a laminar-flow cell culture hood. Upon UV treatment PU films did not shown any visible signs of oxidative damage (such as yellowing), or changes in bulk chemistry ascertained by FTIR spectra, or changes to the micro-pattern or film shape (data not shown).

2.3. Assembly of PU films and EC seeding

Using aseptic techniques, PU films were mounted on the center of autoclaved glass slides (#12-550B, Fisher Scientific, Fairlawn, NJ) using autoclaved high-vacuum grease (Dow Corning, Midland, MI) such that the length of the channels (major axis) would be parallel to the direction of flow as shown in Fig. 1. The film-slide assemblies were placed in 10 cm Petri dishes (Fisher) and the PU (16 mm × 16 mm square) surface was coated with 100 μl of fibronectin (100 μg/ml, BD) in PBS (Gibco, Life Technologies Inc., Carlsbad, CA) and air-dried for 1 hour. Once the liquid had evaporated, the PU-slide assembly was

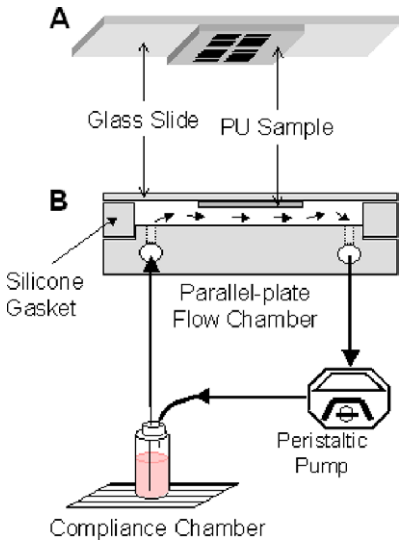

Fig. 1. Schematic representation of the slide assembly (panel A) as well as the flow chamber and perfusion system (panel B). Schematic is not drawn to scale.

bathed in culture medium consisting of DMEM (Cellgro, Herndon, VA), 10% FBS (Hyclone, Logan, UT) and 1% penicillin/streptomycin (Gibco) and left in the incubator for 12 hours until cell seeding. The PU-slide assembly was stored in this manner to prevent desorption of the FN until further use. Bovine aortic endothelial cells (BAEC) at passage 7 to 9 were seeded at 4×10^5 cells per 16 mm $\times$ 16 mm square 24 hours prior to the flow experiment. BAEC on all substrates exhibited cobblestone morphology typical of endothelial cells in a confluent monolayer.

2.4. Flow studies

The flow studies were carried out using a closed-loop perfusion circuit that comprised of a Masterflex roller pump (Model 7553-70, Cole-Parmer, Vernon Hills, IL), compliance chamber (to assure steady flow), parallel-plate flow chamber (Cytodyne, La Jolla, CA and detailed in [8] and a medium reservoir (which was equilibrated with a 5% CO_2 balance air mixture and placed in a 37°C water bath), in series (Fig. 1A). Glass slides containing polymer films seeded with endothelial cells were mounted in parallel-plate flow chambers such that the length of the channels were parallel to flow (Fig. 1B) and then introduced into the flow circuit to expose the films to well-defined laminar fluid flow. PU films seeded with EC were exposed to shear stress for twenty minutes or one hour. The average wall shear stress resulting from steady laminar flow of a Newtonian fluid between two parallel plates can be estimated using the following equation derived for a smooth surface in a parallel-plate flow chamber, $\tau = 6Q\mu/wh^2$, where τ is shear stress in dynes/cm^2, Q is flow rate in ml/s, μ is the viscosity (1 cP), w is width of the parallel plates (2 cm) and, h is the spacing between the parallel plates in cm (0.0490 cm) [8].

2.5. Visualization of cells

At the end of the experiment, cells were fixed in 4% paraformaldehyde (Sigma-Aldrich, St. Louis, MO) for 10 minutes and then cover-slipped with mounting medium containing DAPI (Vector Laboratories, Burlingame, CA). The cells were fixed primarily for two reasons: (1) To ensure longevity of the specimen for image acquisition and analysis and (2) to ensure that the cells do not smear or shrivel up during mounting. Images were acquired using a Zeiss Axiophot microscope (Zeiss, Thornwood, NY) coupled to a CCD camera, with a 5$\times$ objective. Fluorescent micrographs were taken of the center portion of the film for each sample along with a corresponding bright field image to visualize channel outlines. The cells in eight randomly selected images per film were counted manually using a transparency of bright field image as a template. For un-patterned PU, the total number of cells in one image (1.17 mm^2) was counted. For each image of cells on patterned PU, cells were counted separately on 5 plateau and 5 channel regions. Projected areas for these regions were 0.46 ± 0.01 and 0.51 ± 0.01 mm^2, for the plateaus and channels, respectively. Sides of the channels were included in the channel cell and area measurements. Statistical analysis was conducted using JMP-in software (SAS Institute Inc., Cary, NC). Difference in cell density between groups was determined using ANOVA followed by a Tukey–Kramer's HSD post-hoc test with the alpha level set at 0.05.

2.6. Computational fluid dynamics (CFD)

CFD was used to estimate the shear stress in the channel and plateau regions. A 3D model volume was created in pro/ENGINEER (2001, Parametric Technology Corporation) corresponding to the region shown in Fig. 5A. The model volume had a height of 245 μm (half the total spacing, h) and was applicable for regions where entry/exit effects are negligible (e.g., not near the triangular ends of the channel

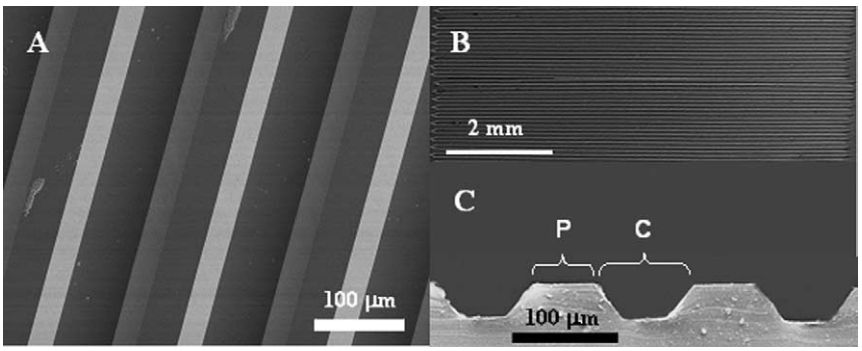

Fig. 2. Scanning electron micrographs of etched silicon wafer (panel A) and cast polyurethane films shown en face (panel B) or cut in cross-section (panel C). The direction of flow is parallel to the long channels shown in panel B. Plateaus and Channels are indicated with P and C, respectively.

visible in Fig. 2B). The maximum fluid velocity was prescribed to the plane at the top of the model geometry, corresponding to a total flow rate of 275 ml/min through the entire flow chamber. Boundary conditions were no-slip for the solid surfaces (i.e., the polymer surface), prescribed velocity for the top surface, straight-out (open to fluid flow) for the front and rear faces, and symmetric for both side surfaces (to eliminate false edge effects). A finite element mesh was automatically generated in FEMLAB and the velocity profile was determined for the model volume by solving the Navier–Stokes equations using FEMLAB's Chemical Engineering Module. From the velocity profile, the shear stress was calculated with the equation $\tau = -\mu \cdot \mathrm{d}v/\mathrm{d}y$ by determining the distance from the surface ($\mathrm{d}y$) at which the velocity was 0.015 m/s ($\mathrm{d}v$).

3. Results

3.1. Characterization of silicon wafer templates and PU films

SEM images of channels in a silicon wafer are shown in Figs 2A and 2B. Wet etching attacks silicon preferentially in the 100 plane, producing a characteristic anisotropic V-shaped etch, with sidewalls that form a 54.7° angle with the surface (35.3° from the normal). Since the silicon wafer is a negative impression of the cast PU films, the channels in the PU correspond to the embossed ridges on the silicon wafer surface (Fig. 2A). The film surface was composed of 4 arrays of channels with each array comprising of a 4 mm × 5 mm rectangle with 31 channels/rectangle (Fig. 2B). Each channel was 32 microns deep, 42 microns wide at its base and 95 microns wide at its top (i.e., plateau-to-plateau distance). Solution casting afforded a simple, reproducible method of transferring the pattern from the silicon wafer to a PU film surface. Under the casting conditions used, films of approximately 160 μm in thickness were obtained. Once the PU films were peeled from the silicon wafer, they retained the complementary micro-patterned features of the silicon template as evidenced by the SEM image of a cross-section of a PU film (Fig. 2C). For sake of simplicity, the channel floor along with its pair of sloping walls will be hitherto referred as the channel and the region between two adjacent channels as the plateau.

3.2. Cell densities under static conditions

BAEC cultured for 24 hours on all PU substrates exhibited cobblestone morphology, typical of endothelial cells in a confluent monolayer (not shown). Cells adhered to all exposed surfaces, including

Table 1

Cell densities (cells/mm^2) based on total and regional areas for un-patterned and patterned surfaces. The cell densities based on total area are calculated by dividing the total number of cells – regardless of whether they are in a plateau or channel – by the total area. The cell densities based on regional areas are calculated by dividing the cell numbers in a given a defined region (e.g., 5 plateaus or 5 channels) by the area of that region. Asterisks (*) represent significance differences between cell densities under flow and static conditions

	Un-patterned PU (total area)	Patterned PU (total area)	Patterned PU (plateau area)	Patterned PU (channel area)
Static	2206 ± 37 ($n = 3$)	2113 ± 292 ($n = 3$)	2104 ± 298 ($n = 3$)	2121 ± 287 ($n = 3$)
Flow	1269 ± 219 ($n = 3$)*	1951 ± 464 ($n = 6$)	1490 ± 328 ($n = 6$)*	2345 ± 320 ($n = 6$)

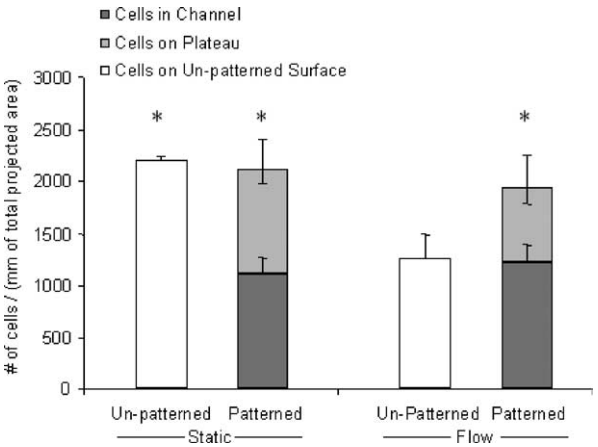

Fig. 3. Cell numbers normalized by *total* projected area for patterned and un-patterned surfaces. As detailed in Methods, for patterned PU, the number of cells was counted separately for the channels and the plateaus and normalized by the sum of project areas of both the channels and plateaus, thus the combined height of the stacked shaded bars gives the total cells density in 1 mm^2 of patterned surface. Flow cultures were exposed to flow with an average wall shear stress of 60 dynes/cm^2 for 1 hour. Error bars represent standard deviation. For upper of the two stacked bars (i.e., to the cells on the plateaus), the negative error bars represent the error associated with the cells on the plateaus and the positive error bars represent the error associated with the sum of the cells on the plateaus and the cells in the channels. An asterisk indicates that the total number of cells on a patterned on un-patterned surface is significant greater ($\alpha < 0.05$) than that of the un-patterned surface exposed to flow. No other differences in total cell numbers approach significance ($\alpha > 0.5$).

the angled channel walls. Under static conditions, the total cell densities for patterned or un-patterned PU were similar, 2113 ± 292 cells/mm^2 or 2206 ± 37 cells/mm^2, respectively (Table 1, Fig. 3). The local cell densities based on projected area in channels and plateaus were also similar (2121 ± 287 and 2104 ± 298 cells/mm^2, respectively), indicating that in static cultures, the presence of the micro-patterned features did not affect the total number of cells or their spatial distribution.

3.3. Shear-stress dose response

Patterned PU substrates ($n = 2$ for each shear stress) were subjected to 10, 20, 40 or 60 dynes/cm^2 for 20 minutes. With shear stresses up to 40 dynes/cm^2, minimal loss of cells occurred on the patterned surface (not shown). With 60 dynes/cm^2, some cell loss from the plateaus was apparent. Based on these observations, a shear stress of 60 dynes/cm^2 was employed in the remainder of this study.

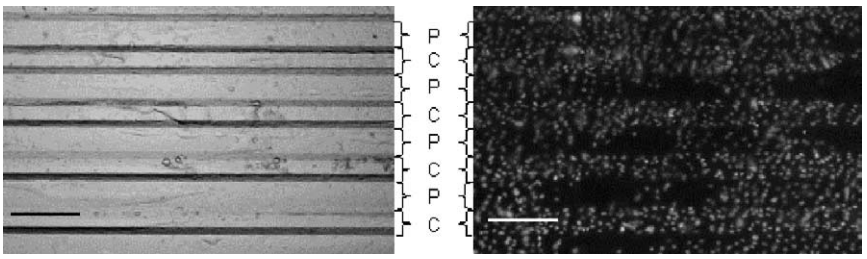

Fig. 4. Phase contrast (panel A) and fluorescent (panel B) micrographs of patterned surfaces that were seeded with cells and exposed to 60 dynes/cm^2 for 1 hour. Channels (C) and Plateaus (P) are visible in light micrographs. Scale bars are 200 microns. The focal plane for acquisition was halfway between the channel bottom and upper edge, to ensure visualization of cells throughout the depth of the channel.

3.4. Effects of micropatterning on BAEC retention

Endothelial cells on patterned and un-patterned PU were exposed to 60 dynes/cm^2 for 1 hr. The number of cells remaining after flow, were determined and the corresponding cell densities were expressed in terms of total projected area (i.e., the total area of the PU surface quantified) and local projected areas (i.e., areas of channel and plateaus). In un-patterned PU exposed to flow, some regions were completely denuded of cells and the total cell density was decreased by 42% (Fig. 3, $\alpha < 0.005$). In contrast, when patterned PU was subjected to the same flow, the total cell density only decreased by 8% (Fig. 3, $\alpha > 0.05$). This improved cell retention was further investigated by considering the cell densities on the channels and plateaus separately. Exposure to flow detached cells from plateaus; overall local cell densities decreased by 29% ($\alpha < 0.05$) with smaller denuded regions (Fig. 4). After exposure to flow, the cell densities on un-patterned surfaces and plateaus were not significantly different. Denuded regions of cells were not seen within the channels. Cell densities within channels remained the same or even increased slightly after exposure to flow (Table 1, Fig. 3, 11% increase in cell density is not significant). As hypothesized, micropatterning the surface increased the total number of cell retained after flow, primarily by increasing the number of cells retained within the channels (Fig. 3).

3.5. Simulation of flow in channels in patterned PU surfaces

The 3D model channel geometry used in the simulation studies was converted into a finite element mesh with 611 nodes and 2206 elements for the channel model. The velocity profiles for fluid flow in both the model patterned surface (Fig. 5A–C) and the model un-patterned surface (not shown) were determined using FEMLAB. The solution was determined from 0–10 seconds, and found to not vary with time, suggesting the solution had reached steady state. From the velocity profile, shear stresses were calculated for the patterned and un-patterned surfaces (Fig. 5C, solid line and dotted horizontal line, respectively). The average shear stress over the entire modeled patterned surface including the plateau and channel was 61.1 dyn/cm^2, similar to the average of the un-patterned surface (63.2 dyn/cm^2). The average shear stress for the entire channel (45.8 dyn/cm^2) was 27.6 % less than the average shear stress of the un-patterned surface, with the average shear stress on the channel floor (25.1 dyn/cm^2) was reduced more than that of the channel side-walls (56.3 dyn/cm^2). The average shear stress of the plateau regions (98.5 dyn/cm^2) was 55.6 % greater than the shear stress of the control model, while the average stress on the side-walls of the channel was only somewhat reduced (10.9 %).

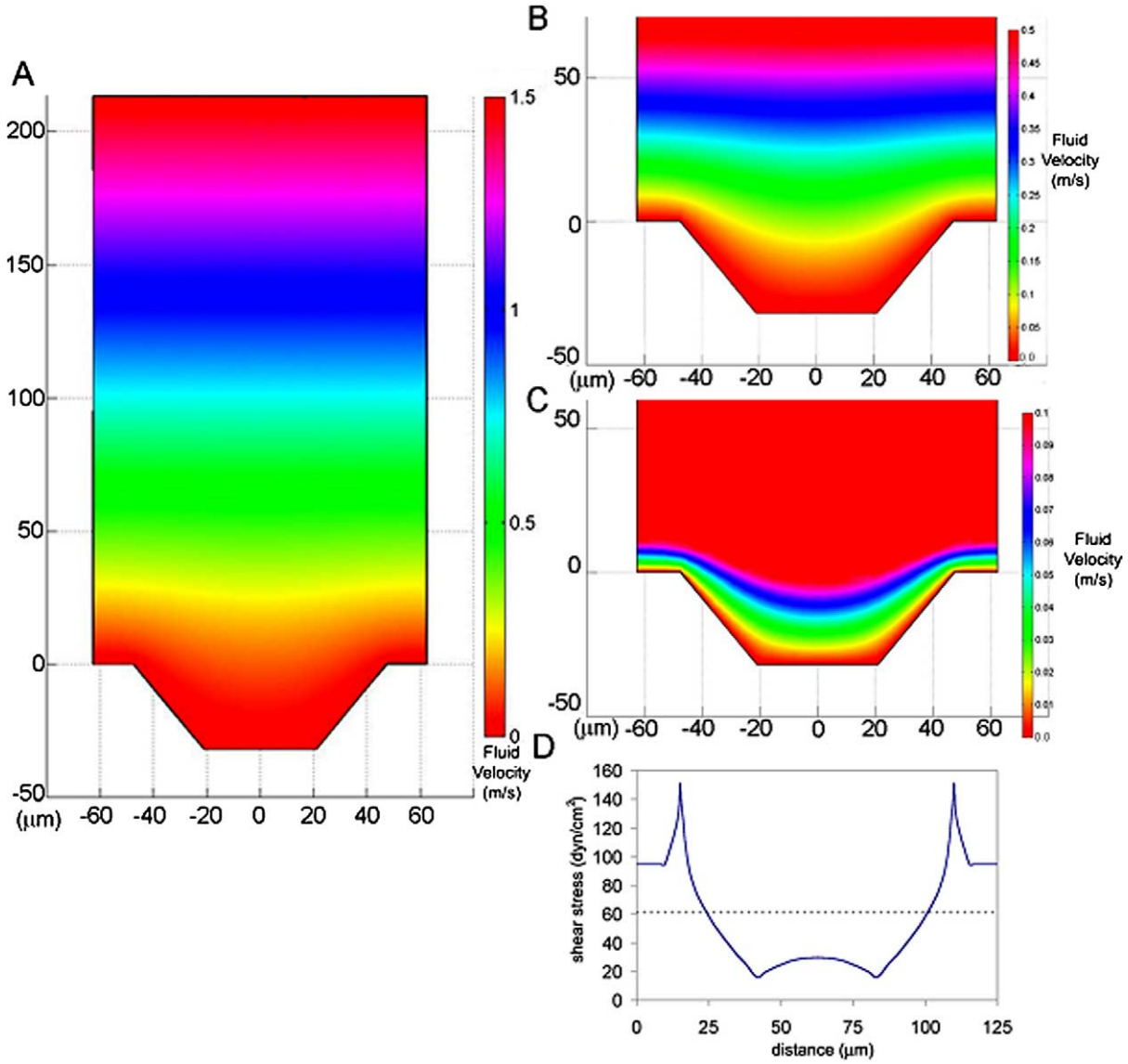

Fig. 5. Computational fluid dynamics simulation of velocity profile and wall shear stress for micro-patterned surfaces corresponding to those used for endothelial retention studies: For the regions relatively far from the polyurethane surface, the velocity varied linearly with vertical distance (panel A). Closer to the polyurethane surface, the velocity profile was altered by the presence of the channel (panels B and C) resulting in reduced wall shear stress within the channel and increased wall shear stress in the plateau region (panel D, solid line). Note the average wall shear stress for the patterned surface (61 dyne/cm^2) was nearly identical to the wall shear stress calculated for an un-patterned surface with the same bulk flow (panel D, dashed line).

CFD offers the potential to rapidly explore the effects of changing channel geometry and shape and thus could aid in the rational design of patterned surfaces. For instance, using the same fluid boundary conditions and fluid velocity, models were created that investigated the effects of increasing or decreasing overall channel depth (Fig. 6A, C) and width (Fig. 6B, D). The depth of the channel was varied from that of the physical model (32 μm, Fig. 6A, black line), by either increasing (40 μm, Fig. 6A, gray line), or decreasing (24 μm, Fig. 6A, dashed line) by 8 μm or 25% of the original depth, without

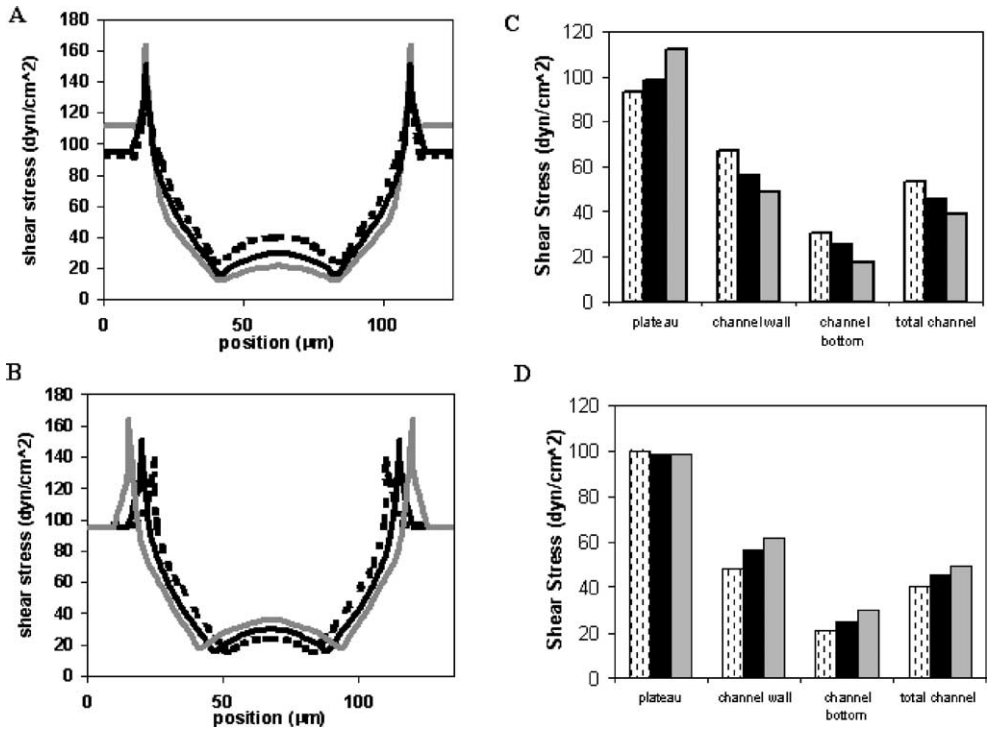

Fig. 6. Computational fluid dynamics simulation of the effects of changing channel depth (panels A and C) or changing channel width (panels B and D): Increasing the depth of the channel by 25% (gray line and bar, panels A and C) from the actual geometry used for endothelial retention studies (black line and bar, panels A and C) had the effect of increasing the wall shear stress in the plateau region, but decreasing the wall shear stress throughout the wall and channel. Decreasing the depth by a similar amount (dashed line and bar, panels A and C) had an opposite effect. Increasing the width of the channel by 10 μm (gray line and bar, panels B and D) from the actual geometry used in endothelial retention studies (black line and bar, panels B and D) increased the shear stress throughout the channel, without affecting the shear stress in the plateau regions. Similarly decreasing the width by 10 μm (dashed line and bar, panels B and D) had an opposite effect in the channel region, without affecting the plateau region.

altering the width of either the overall channel, or the bottom surface. Increasing the channel depth, and the associated plateau-channel junction angle, increased both the peak shear stress and average plateau shear stress, while decreasing the shear stress throughout the channel (Fig. 6C). To further investigate the effects of channel geometry, the width of the bottom surface of the channel was varied from the actual width of the physical model (42 μm, Fig. 6B, black line), by either increasing (52 μm, Fig. 6B, gray line) or decreasing (32 μm, Fig. 6B, dashed line) by 10 μm, without altering any other aspect of the geometry or the fluid flow conditions. Increasing the channel width increased the peak shear stress at the plateau-channel junction but not the average plateau shear stress, while increasing the shear stress throughout the channel (Fig. 6D).

4. Discussion

The idea that endothelial cells within local micro-domains with reduced flow-induced shear are more resistant to flow-induced cell loss is conceptually simple. This concept may partially explain the observations of others that when elevated transmural pressures is used to "sod" endothelial cells onto a graft, which forces some of the cells up to 50 microns into pores in the graft, the retention of cells following

exposure to flow is increased (e.g., [5]). Though conceptually simply and potentially useful for explaining existing experimental observations, to our knowledge our work is the first well-controlled evaluation of this concept or attempt to systematically exploit it to improve endothelial cell retention.

As hypothesized, EC retention was increased in channels, which were exposed to reduced shear stress relative to un-patterned surfaces subjected to the same bulk flow rate. Importantly, this improvement in the channels did not come at the expense of decreased EC retention on the plateaus relative to un-patterned surface, despite an increase in shear stress on the plateaus. One possible reason for improved endothelial retention on the plateaus relative to the un-patterned surfaces is that patterning appears to have prevented larger patches of denudation, which tended to occur on un-patterned surfaces. It is reasonable to assume that the presence of the protected channels may have prevented the propagation of denuded patches and thereby limited the cell loss in the plateaus by this mechanism. It is also possible that cells residing on the edges of plateaus were further anchored by attachment to cells in the valleys. By improving EC retention in the channels, micro-patterning increased the total number of EC retained on the graft surface. Of potential concern could be that the remaining EC are preferentially subjected to reduced shear stress, which may conceivably diminish their production of anti-thrombogenic compounds [7,9]. Edelman, however, demonstrated EC could have positive effects on vessel health even when they were seeded on the adventitial surface of a vessel and thus not in contact with any flow [14].

Due to the ease with which micropattern configurations can be generated, we believe they can be readily optimized. For example, extensions of the micropattern configuration explored in this study can be generated by changing the depth, width, shape, spacing and orientation of the channels. The affects of theses changes on shear stress distributions could be rapidly assessed using CFD and the ability of promising designs to support EC retention could be evaluated experimentally. In addition, correlating endothelial cell adhesion with shear stress predictions for multiple micropattern configurations would be necessary before definitively attributing the improved cell retention to micropattern-associated reduction in shear stress rather than factors such as feature geometry and dimensions that are associated with surface topology. Ideally, one would like to design a surface pattern that would significantly reduce the total shear force exerted over the entire luminal surface, but mechanical constraints prevent realization of this goal. Specifically, a simple force balance on the volume of fluid in a conduit of constant diameter dictates that the shear force exerted along the walls of the conduit must balance the pressure drop times the cross-sectional area of the fluid. Since surface texture has only a negligible effect on the pressure drop of laminar flow through a conduit, the total shear force exerted on the luminal surface therefore is not affected by the micropatterning. A corollary to this statement is that if micropatterning decreases the total shear force applied to one set of regions (e.g., the channels), it must increase the total force applied to another (e.g., the plateaus). A modest decrease in average shear stress, however, is possible as micropatterning can increase the area over which the total shear force is applied. These considerations coupled with the experimental data suggest that the primary mechanism by which micropatterning improves EC retention is by lowering shear stresses in local regions and not average shear stress over the entire lumen surface.

Here we present encouraging results with respect to EC retention using a non-chemical approach based on creating micropatterns by solvent casting of a synthetic polymer onto a surface etched silicon mold. As summarized earlier, several studies have reported chemical modification strategies that improve EC retention on various polymer surfaces. A significant benefit of the non-chemical approach presented here is that using simple techniques such as solvent casting or high-pressure imprinting, well-defined micropatterns can be generated on virtually any surface including Teflon (Gore-Tex). Furthermore, the micropatterning strategy can be combined with chemical modification approaches to further enhance EC retention.

Acknowledgements

This work was supported in part by NIH (R24-AI47739-03, sub-award to VPS, R01 HL 64388-01A1 to KJG) and a Whitaker pre-doctoral award to ALS. The authors also wish to thank Vladimir Dominko at the PENN micro-fabrication facility for assistance with wafer fabrication.

References

[1] M. Baguneid et al., Shear-stress preconditioning and tissue-engineering-based paradigms for generating arterial substitutes, *Biotechnol. Appl. Biochem.* **39** (2004), 151–157.
[2] G.L. Bowlin et al., In vitro evaluation of electrostatic endothelial cell transplantation onto 4 mm interior diameter expanded polytetrafluoroethylene grafts, *J. Vasc. Surg.* **27** (1998), 504–511.
[3] S.J. Brener et al., Propensity analysis of long-term survival after surgical or percutaneous revascularization in patients with multivessel coronary artery disease and high-risk features, *Circulation* **109** (2004), 2290–2295.
[4] H.M. Carr et al., Endothelial cell seeding kinetics under chronic flow in prosthetic grafts, *Ann. Vasc. Surg*. **10** (1996), 469–475.
[5] B.P. Chan et al., In vivo performance of dual ligand augmented endothelialized expanded polytetrafluoroethylene vascular grafts, *J. Biomed. Mater. Res. B Appl. Biomater.* **72** (2005), 52–63.
[6] A. Dardik, A. Liu and B.J. Ballermann, Chronic in vitro shear stress stimulates endothelial cell retention on prosthetic vascular grafts and reduces subsequent in vivo neointimal thickness, *J. Vasc. Surg.* **29** (1999), 157–167.
[7] S.L. Diamond, S.G. Eskin and L.V. McIntire, Fluid flow stimulates tissue plasminogen activator secretion by cultured human endothelial cells, *Science* **243** (1989), 1483–1485.
[8] J. Frangos, L. Mcintire and S. Eskin, Shear-stress induced stimulation of mammalian-cell metabolism, *Biotechnology and Bioengineering* **32** (1988), 1053–1060.
[9] K.J. Gooch and J.A. Frangos, Flow- and bradykinin-induced nitric oxide production by endothelial cells is independent of membrane potential, *Am. J. Physiol.* **270** (1996), C546–C551.
[10] T.V. How and R.M. Clarke, The elastic properties of a polyurethane arterial prosthesis, *J. Biomech.* **17** (1984), 597–608.
[11] S.H. Hsu, S.H. Sun and D.C. Chen, Improved retention of endothelial cells seeded on polyurethane small-diameter vascular grafts modified by a recombinant RGD-containing protein, *Artif. Organs.* **27** (2003), 1068–1078.
[12] H.B. Lin et al., Endothelial cell adhesion on polyurethanes containing covalently attached RGD-peptides, *Biomaterials* **13** (1992), 905–914.
[13] S.P. Massia and J.A. Hubbell, Human endothelial cell interactions with surface-coupled adhesion peptides on a nonadhesive glass substrate and two polymeric biomaterials, *J. Biomed. Mater. Res.* **25** (1991), 223–242.
[14] H.M. Nugent and E.R. Edelman, Endothelial implants provide long-term control of vascular repair in a porcine model of arterial injury, *J. Surg. Res.* **99** (2001), 228–234.
[15] S.J. Stachelek et al., Cholesterol-derivatized polyurethane: characterization and endothelial cell adhesion, *J. Biomed. Mater. Res. A.* **72A** (2005), 200–212.
[16] K.P. Walluscheck et al., Improved endothelial cell attachment on ePTFE vascular grafts pretreated with synthetic RGD-containing peptides, *Eur. J. Vasc. Endovasc. Surg.* **12** (1996), 321–330.
[17] H. Yu et al., Smooth muscle cells improve endothelial cell retention on polytetrafluoroethylene grafts in vivo, *J. Vasc. Surg.* **38** (2003), 557–563.
[18] P. Zilla and H. Greisler, *Tissue Engineering of Vascular Prosthetic Grafts*, R.G. Landes Company, Austin, 1999.